42–52 *Nucleic Acids Research, 2006, Vol. 34, No. 1*
doi:10.1093/nar/gkj411

Mg^{2+} dependency of HIV-1 reverse transcription, inhibition by nucleoside analogues and resistance

Valérie Goldschmidt, Joël Didierjean, Bernard Ehresmann, Chantal Ehresmann, Catherine Isel and Roland Marquet*

Unité Propre de Recherche 9002 du CNRS conventionnée à l'Université Louis Pasteur, IBMC, 15 rue René Descartes, 67084 Strasbourg cedex, France

Received August 26, 2005; Revised and Accepted December 7, 2005

ABSTRACT

Metal ions are essential for DNA polymerase and RNase H activities of HIV-1 reverse transcriptase (RT). RT studies are routinely performed at 6–8 mM Mg^{2+}, despite the fact that the *in vivo* concentration might be as low as 0.2 mM. We studied the influence of $MgCl_2$ and ATP, which likely binds a significant fraction of the magnesium pool *in vivo,* on the DNA polymerase and RNase H activities of HIV-1 RT, its inhibition by nucleoside RT inhibitors (NRTIs) and primer unblocking by AZT-resistant RT. At low Mg^{2+} concentration, reverse transcription of a natural template strongly increased despite a dramatically reduced intrinsic polymerase activity under such conditions. Low Mg^{2+} concentrations affected the RNA stability and indirectly decreased its degradation by the RNase H activity. The reduced RNA degradation prevented premature dissociation of the template and primer strands that otherwise generated dead-end DNA products. In addition, low Mg^{2+} dramatically decreased the incorporation of NRTIs into DNA and increased nucleotide excision by AZT-resistant RT. The latter effect is also most likely owing to the diminished cleavage of the RNA template. Thus, differences in the free Mg^{2+} concentration between different cell types or during the cell cycle might strongly affect HIV-1 replication and its inhibition.

INTRODUCTION

Reverse transcriptase (RT) is a key enzyme in the life cycle of human immunodeficiency virus type 1 (HIV-1) and one of the main targets of antiviral therapy [reviewed in (1,2)]. Its DNA polymerase and RNase H functions are essential for synthesis of the proviral DNA (1). Both the catalytic sites bind metal ions (most likely Mg^{2+} *in vivo*). Two Mg^{2+} ions separated by ~3.6 Å have been observed in the polymerase active site of RT in complex with a primer/template DNA duplex and an incoming nucleotide (3). The three aspartate residues that bind Mg^{2+} (D110, D185 and D186) and the metal ions themselves are essential for DNA synthesis (4,5). Divalent metal ions are also essential for HIV-1 RNase H activity (6), but the number of ions involved in the RNA cleavage reaction is still unclear [(7) and references therein]. Two Mn^{2+} ions separated by ~4 Å have been observed in the isolated HIV-1 RNase H domain (8), whereas only one Mg^{2+} ion was seen in the RNase H domain of RT bound to a DNA duplex, in the presence of an incoming dNTP (3). However, the recent crystal structures of wild type (wt) and catalytically inactive bacterial RNase H complexed with RNA/DNA hybrids showed that the four carboxylate residues of the catalytic site bind two Mg^{2+} ions separated by 4.1–4.4 Å (9).

Despite this fact, the influence of the Mg^{2+} concentration on reverse transcription is not well documented. With homopolymeric RNA templates, HIV-1 RT polymerase and RNase H activities were found to be optimal at 3–8 mM and 4–12 mM Mg^{2+}, respectively (10–13), but the effect of the magnesium concentration on reverse transcription of natural RNA templates remains largely unknown. RT studies are routinely performed at 6–8 mM Mg^{2+}, despite the fact that the *in vivo* magnesium concentration might be significantly lower: for instance, the Mg^{2+} concentration is 0.21–0.24 mM in the brain (14), ranges from 0.25 to 0.75 mM in blood (15) and is 0.24 ± 0.03 mM in human lymphocytes, one of the main HIV-1 targets (16). In addition, most intracellular magnesium is bound to DNA, RNA, dNTP and NTP [of which ATP is the most abundant: the intracellular ATP concentration is typically between 1.3 and 4.3 mM (16,17)], and the critical parameter is likely the concentration of free Mg^{2+} ions.

Nucleoside RT inhibitors (NRTIs) constitute one of the main classes of anti-HIV drugs [reviewed in (2,18)], but little is known about the influence of the Mg^{2+} concentration on

*To whom correspondence should be addressed. Tel: +33 3 88 41 70 54; Fax: +33 3 88 60 22 18; Email: r.marquet@ibmc.u-strasbg.fr

their incorporation efficiency. Since the Mg^{2+} ions of the polymerase active site do not interact with the 3′ hydroxyl group of the incoming dNTP (3), the Mg^{2+} concentration is not expected to be a major determinant of the NRTI efficiency. However, it was shown that AZTTP and d4TTP require higher Mg^{2+} concentration than dTTP for optimal incorporation, pointing at the importance of this parameter (19).

As for other antiviral drugs, prolonged treatments with NRTIs select for mutations in the RT gene that confer resistance to these nucleoside analogues (2,18). These mutations decrease the incorporation of the chain terminators into DNA or/and favor primer unblocking by excision of incorporated NRTIs (20). Both the resistance mechanisms might potentially be affected by the magnesium concentration. However, this has not been studied to date.

Here, we studied reverse transcription of a natural RNA template, its inhibition by NRTIs, primer unblocking by AZT-resistant RT, as well as RNase H activity, at different magnesium concentrations, in the presence or absence of physiological ATP concentration. We found that the concentration of free Mg^{2+} ions has dramatic effects on these reactions. Thus, differences in the free Mg^{2+} concentration between different cell types or during the cell cycle might strongly affect HIV-1 replication and its inhibition by NRTIs. In addition, our results have important implications for screening and testing of candidate NRTIs.

MATERIALS AND METHODS

ODN, an 18mer DNA complementary to the primer binding site (PBS), was chemically synthesized and 5′ end-labeled with [γ^{32}P]ATP and polynucleotide kinase from phage T4. The template RNA, encompassing 1–311 nt of HIV-1 MAL genomic RNA, was transcribed *in vitro* and purified as described in (21). A plasmid expressing wt HIV-1 RT was kindly provided to us by Dr Torsten Unge (Uppsala, Sweden), together with the protocols for protein overexpression and purification. RNase H(−) HIV-1 RT bearing the E478Q point mutation, AZT-resistant RT bearing mutations D67N, K70R, T215F and K219Q, and 3TC-resistant RT bearing mutation M184V were purified essentially as described in (22). AZTTP, d4TTP and 3TCTP stock solutions were obtained from Moravek Biochemicals and treated with 0.5 U of pyrophosphatase (Roche Molecular Biochemicals) for 1 h at 37°C in 100 µl of 50 mM Tris–HCl, pH 8.0, 50 mM KCl, 6 mM $MgCl_2$ and 1 mM DTT, in order to prevent contamination with PPi. Pyrophosphatase was removed by filtration through a Centricon 10 (Amicon) device.

Determination of the RT activity on poly(rA) template was performed as follows. Poly(rA)/$(dT)_{18}$ (500 nM) was extended by 25 nM wt RT in the presence or absence of 3.5 mM ATP and 1 µM [^{3}H]dTTP and various $MgCl_2$ concentrations. Aliquots were withdrawn every minute during 5 min and analysed on a 96 well filtration unit (MultiScreen$_{HTS}$ Vacuum Manifold; Millipore). The fiber glass membranes (Millipore) were pre-incubated at 4°C with 100 µl of 5% TCA, and the samples were further incubated in TCA for 30 min. After filtration, the membranes were washed twice with 100 µl ice-cold 5% TCA and once with ethanol. The membranes were dried, placed into 2 ml of Ecoscint OTM, and radioactivity was counted. For each $MgCl_2$ concentration, the initial velocity (V_i) was determined by plotting the amount of incorporated radioactivity versus time.

For ssDNA synthesis, template RNA and ^{32}P-labeled ODN were denatured in water for 2 min at 90°C, chilled on ice and incubated at 70°C for 20 min in 50 mM sodium cacodylate (pH 7.5) and 300 mM KCl. The annealing efficiency was routinely checked by native 8% polyacrylamide gel electrophoresis. The primer/template complex (10 nM final concentration) and the four dNTPs (50 µM each) were pre-incubated for 4 min at 37°C in 50 mM Tris–HCl pH 8.0, 50 mM KCl, 1–6 mM $MgCl_2$, 1 mM DTE, with or without 3.5 mM ATP, AMP, EDTA or EGTA. Reverse transcription was initiated by adding 25 nM RT in the same buffer. DNA synthesis was stopped at different time intervals by adding an equal volume of formamide containing 50 mM EDTA. To study the inhibition of reverse transcription by NRTIs, DNA synthesis was performed in presence of 4 or 5 µM of AZTTP, d4TTP, 3TCTP, ddCTP or ddATP. The products were analysed on 15% denaturing polyacrylamide gels and quantified with a BioImager BAS 2000 (Fuji).

Two polymerase-dependent RNase H assays were performed. The first one has been recently described elsewhere (23). Briefly, a 5′ end-labeled RNA template encompassing nt 1–47 of HIV genomic RNA (RNA1-47) was annealed to a DNA oligonucleotide (ODN35), and 10 nM of ODN35/RNA1-47 complex were added to 10 nM wt HIV-1 RT in 50 mM Tris–HCl, pH 8.0, 50 mM KCl, 1–6 mM $MgCl_2$, 1 mM DTE, with or without 3.5 mM ATP. RNase H cleavage was carried out for 15 s to 30 min and stopped by mixing with an equal volume of formamide containing 50 mM EDTA. Cleavage products were resolved using denaturing 15% polyacrylamide gels and quantified as described above. The cleavage rate constants were determined by fitting the experimental data to an exponential equation. In the second assay, we used unlabeled ODN annealed to 5′ end-labeled RNA1-311, and we directly followed cleavage of the RNA template during ssDNA synthesis, which was performed as described above.

RESULTS AND DISCUSSION

Influence of ATP and Mg^{2+} on the RT polymerase activity

The main goal of this study was to examine the influence of the free Mg^{2+} concentration on reverse transcription of a natural RNA template. However, as we expected Mg^{2+} to have pleotropic effects on the polymerase and RNase H RT activities and on the structure and stability of the RNA template, we first analysed the RT polymerase activity on poly(rA), which is devoid of secondary structure.

We performed steady-state kinetics of reverse transcription of poly(rA) at various $MgCl_2$ concentrations, ranging from 1 to 10 mM, in the absence and presence of 3.5 mM ATP, which is likely the main intracellular Mg^{2+} ligand. This ATP concentration is intermediate between that found in human lymphocytes (4.3 mM) (16) and other human cell lines such as H9 cells, macrophages, and unstimulated $CD4^+$ or $CD8^+$ T cells (1.3–2.2 mM) (17). For each ionic condition, we determined the initial velocity (V_i) of reverse transcription.

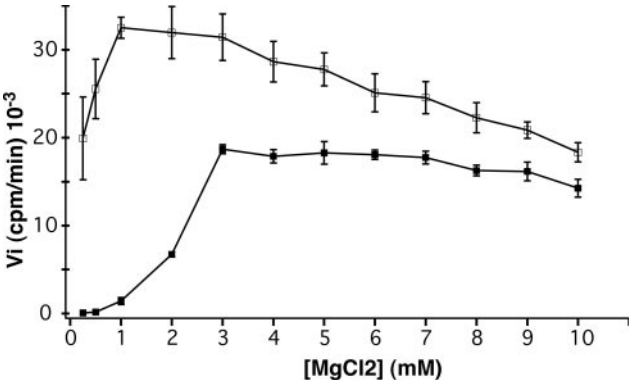

Figure 1. Influence of the $MgCl_2$ concentration on the rate of poly(rA) reverse transcription in the absence and in the presence of ATP. Poly(rA)/$(dT)_{18}$ (500 nM) was extended by 25 nM wt RT with 1 μM [^{3}H]dTTP at various $MgCl_2$ concentrations, with (closed squares) or without (open squares) 3.5 mM ATP. For each condition, the initial velocity (V_i) was determined as described in Materials and Methods and plotted versus the $MgCl_2$ concentration.

For homopolymeric templates, V_i is directly proportional to the incorporation rate of a single nucleotide.

In the absence of ATP, V_i was maximum at 1 mM $MgCl_2$, smoothly decreased as the Mg^{2+} concentration increased up to 10 mM and abruptly decreased below 1 mM $MgCl_2$ (Figure 1). As the stability of RT/nucleic acid complexes is highly sensitive to salts (24), we suggest that the polymerase activity decrease above 1 mM $MgCl_2$ owes to faster dissociation of the enzyme as the ionic strength increases. Previous studies with HIV-1 RT and homopolymeric RNA also reported smooth variations of the polymerase activity between 1 and 10 mM Mg^{2+}, but the RT activity was usually optimum at ~5 mM $MgCl_2$ (10,11,13). However, most of these studies were performed at lower salt concentration than our experiments. Thus, higher $MgCl_2$ concentration was likely required to dissociate the RT/nucleic acid complexes. In addition, in these studies HIV-1 RT was purified from viral particles, and these protein samples probably contained Ca^{2+} traces (10). Low concentrations of this cation strongly inhibit HIV-1 RT and shift the apparent Mg^{2+} dependency of the polymerase activity to higher concentration (25). Using recombinant HIV-1 RT, Tan *et al*. (25) showed that the optimal $MgCl_2$ concentration for polymerase activity was 1–2 mM in the absence of Ca^{2+} and 8–12 mM in the presence of ~50 μM Ca^{2+}, in good agreement with our results.

The sharp polymerase activity decrease below 1 mM $MgCl_2$ is most likely directly linked to binding of the Mg^{2+} ions in the catalytic site. The RT polymerase site contains two Mg^{2+} ions when bound to a DNA duplex in the presence of an incoming nucleotide (3). One of the Mg^{2+} ions (MgB) is bound to the three phosphate groups of the incoming dNTP and to catalytic D110 and D185 (3). This ion is brought into the catalytic site by the incoming nucleotide, and its tight binding likely prevents significant exchange with free NTP and dNTP. The second ion (MgA) binds the three catalytic Asp residues and the α-phosphate of the incoming dNTP. This catalytic ion is not bound in the RT polymerase site in the absence of the incoming dNTP (26), and a recent study on HIV-1 RT indicated that its association constant is in the millimolar range (1.5 mM) (19). Thus, millimolar concentrations of Mg^{2+} ions are required to saturate the RT polymerase site, in agreement with our experimental data.

Table 1. Influence of the Mg^{2+} concentration on the synthesis of (−) strand strong stop DNA

[Total Mg^{2+}] (mM)	1	2	3	4	5	6
(−) Strand strong stop DNA (%)[a]						
−ATP	20	17	15	13	12	12
+ATP	27	32	29	21	18	17
[Free Mg^{2+}] (mM)[b]	0.02	0.1	0.3	0.8	1.7	2.6

[a]([(−) strong stop DNA]/[extended + unextended primer]) × 100.
[b]Calculated concentration of free Mg^{2+} ions in the presence of 3.5 mM ATP.

When we studied reverse transcription of poly(rA) in the presence of 3.5 mM ATP, V_i smoothly decreased between 3 and 7 mM $MgCl_2$ and sharply dropped below 3 mM (Figure 1). Thus, addition of 3.5 mM ATP shifted the optimal $MgCl_2$ concentration from 1 to 3 mM, strongly suggesting that ATP is able to compete with the RT polymerase site for the binding of Mg^{2+} ions. Indeed, the affinity of Mg^{2+} is at least one order of magnitude greater for ATP ($K_a = 10^{4.05}$ M^{-1}) than for the RT polymerase site ($K_a = 10^{2.82}$ M^{-1}, see above). In addition, the polymerase activity was systematically lower in the presence of ATP, suggesting that owing to its large excess, this nucleotide might compete with dTTP for the RT catalytic site.

Influence of Mg^{2+} on (−) strand strong stop DNA synthesis

To study the effects of the Mg^{2+} concentration on reverse transcription of a natural template, we used an RNA encompassing 1–311 nt of HIV-1 genomic RNA (MAL isolate), and followed the synthesis of (−) strand strong stop DNA (ssDNA) from a DNA primer bound to the PBS. Reverse transcription was performed at $MgCl_2$ concentrations ranging from 1 to 6 mM, in the absence and in the presence of 3.5 mM ATP. Given the stability of the Mg^{2+}/ATP complex ($K_a = 10^{4.05}$ M^{-1}), we calculated that in the presence of 3.5 mM ATP, the concentration of free Mg^{2+} ions ranged from 0.02 to 2.6 mM (Tables 1 and 3).

In the absence of ATP, synthesis of ssDNA was most efficient at 1 mM $MgCl_2$, gradually decreased as the $MgCl_2$ concentration increased and reached a plateau at 4–6 mM $MgCl_2$ (Table 1). Remarkably, ssDNA synthesis was strongly improved in the presence of 3.5 mM ATP (Table 1). Importantly, similar ssDNA levels were obtained at comparable concentrations of free Mg^{2+} ions (e.g. at 2 mM $MgCl_2$ without ATP and 6 mM $MgCl_2$ with ATP, or at 1 mM $MgCl_2$ without ATP and 4 mM $MgCl_2$ with ATP, see Table 1), strongly suggesting that the effect of ATP was due to chelation of Mg^{2+}. Surprisingly, synthesis of ssDNA was optimal at 0.1 mM free Mg^{2+} and was still very efficient at 20 μM free Mg^{2+} (Table 1), in contrast with the polymerase activity measured on poly(rA) (Figure 1). Similar results were obtained with AZT-resistant RT (bearing mutations D67N, K70R, T215F and K219Q) and 3TC-resistant RT (bearing mutation M184V) (data not shown).

To confirm that the effect of ATP was due to chelation of Mg^{2+} ions, we substituted EDTA, EGTA or AMP for ATP (Table 2). At pH 8, EDTA binds Mg^{2+} ions ~200-fold more

Table 2. Influence of ATP, EGTA, EDTA and AMP on the synthesis of (−) strand strong stop DNA

[$MgCl_2$] (mM)		−	+ATP	+EGTA	+EDTA	+AMP
2	(−) Strand strong stop DNA (%)[a]	17	29	25	0	19
	[Free Mg^{2+}] (mM)[b]	2	0.1	0.7	0.0005	1.7
6	(−) Strand strong stop DNA (%)[a]	11	19	18	17	11
	[Free Mg^{2+}] (mM)[b]	6	2.6	3.5	2.5	5.1

[a]([(−) strong stop DNA]/[extended + unextended primer]) × 100.
[b]Calculated concentration of free Mg^{2+} ions in the presence of 3.5 mM ATP, EGTA, EDTA or AMP.

Table 3. Influence of the Mg^{2+} concentration on the inhibition of ssDNA synthesis by NRTIs

	(−) Strand strong stop DNA (%)[a]			
	6 mM Mg^{2+}	6 mM Mg^{2+} + 3.5 mM ATP[b]	2 mM Mg^{2+}	2 mM Mg^{2+} + 3.5 mM ATP[c]
No NRTI	12 10[d]	17	17	34 29[d]
ddATP	1.3 0[d]	3.8	3.5	29 16[d]
ddCTP	1.1	1.1	2.6	24
3TCTP	5.4	10	8.9	27
d4TTP	1.8	2.8	3.2	21
AZTTP	0.05 0[d]	0.11	0.31	13 8[d]

[a]([(−) strong stop DNA]/[extended + unextended primer]) × 100.
[b]The calculated free Mg^{2+} concentration is 2.6 mM.
[c]The calculated free Mg^{2+} concentration is 0.1 mM.
[d]These experiments were performed with RNase H(−) RT.

efficiently than ATP ($K_a = 10^{6.43}$), whereas EGTA is a poorer Mg^{2+} ligand ($K_a = 10^{2.84}$) and AMP does not significantly bind Mg^{2+} ions ($K_a = 10^{1.8}$). At 6 mM $MgCl_2$, ATP, EGTA and EDTA significantly increased ssDNA synthesis, while AMP did not, in agreement with their chelating capacities (Table 2). At 2 mM $MgCl_2$, EGTA increased ssDNA synthesis, but to a lower extend compared with ATP (Table 2), in agreement with our previous observation that ssDNA synthesis was optimal at ∼0.1 mM free Mg^{2+} (Table 1). On the other hand, no ssDNA synthesis was observed with EDTA, suggesting that the very low concentration of free Mg^{2+} ions was not sufficient to catalyse incorporation of dNTPs (Table 1). Accordingly, only very short DNA products were observed under these conditions (data not shown). Finally, AMP had very little influence on ssDNA synthesis. Taken together, these results indicate that the effect of ATP on ssDNA synthesis is mainly due to chelation of Mg^{2+} ions.

Looking at both the plateau and kinetics of ssDNA synthesis at various $MgCl_2$ and ATP concentrations, we observed that the free Mg^{2+} concentration had little effect on the rate of ssDNA synthesis: in all cases, ssDNA reached a plateau after ∼12 min (Figure 2). However, the free Mg^{2+} concentration strongly affected the value of this plateau (Figure 2 and Table 1), suggesting that the RNA structure, rather than the intrinsic catalytic efficiency of RT, influenced ssDNA synthesis. Indeed, unlike poly(rA) and other homopolymeric

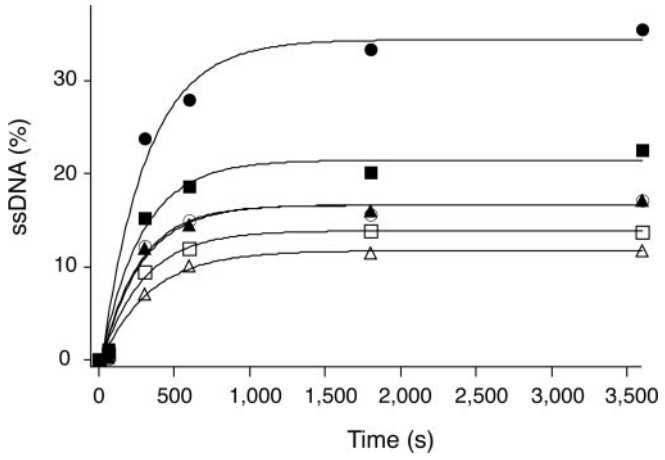

Figure 2. Influence of $MgCl_2$ and ATP on ssDNA synthesis. Kinetics of ssDNA synthesis at 2 (circles), 4 (squares) or 6 (triangles) mM $MgCl_2$, in the absence (open symbols) or in the presence (closed symbols) of 3.5 mM ATP.

RNAs, the 5′ region of HIV-1 genomic RNA fold into several stem–loop structures whose stability is Mg^{2+}-dependent (27,28).

Influence of Mg^{2+} on formation of dead-end reverse transcription products

During ssDNA synthesis, several strong bands corresponding to intermediate products appear between the primer and the full-length ssDNA (Figure 3). Analysis of the reverse transcription products indicated that ATP enhanced reverse transcription of HIV-1 RNA mainly by preventing accumulation of these intermediate bands (Figure 3A). At least two classes of intermediate products can be distinguished. The first class includes the bands (indicated by open stars in Figure 3) that decreased over time, even in the absence of ATP: these are 'true' intermediate products. They were most likely due to a transient block of RT by stable RNA structures that were ultimately unfolded and reverse transcribed, as previously observed (29–31). Expectedly, pausing at these positions decreased when the RNA structure was destabilized by lowering the free Mg^{2+} concentration (Figure 3A).

The second class includes very strong bands (some of which are indicated by black stars in Figure 3A) that did not decrease with increasing reaction times, indicating that they correspond to abortive (dead-end) products. Interestingly, the amount of some of these dead-end products (indicated by black stars in Figure 3A), but not all, strongly decreased in the presence of ATP, especially at low $MgCl_2$ concentration. A possibility is that, at these positions, the RNA template was rapidly cut during a polymerization arrest and dissociated from the elongating DNA strand before RT could pass through the stop. A low free Mg^{2+} concentration could destabilize the RNA structure, thus preventing the polymerase block, or/and decrease the intrinsic RNase H activity (Figure 3A, right panel).

RNase H activity and ssDNA synthesis

To test whether accumulation of dead-end products required RNase H activity, we used E478Q RNase H(−) RT. At 2 mM $MgCl_2$, almost no dead-end product was apparent with this

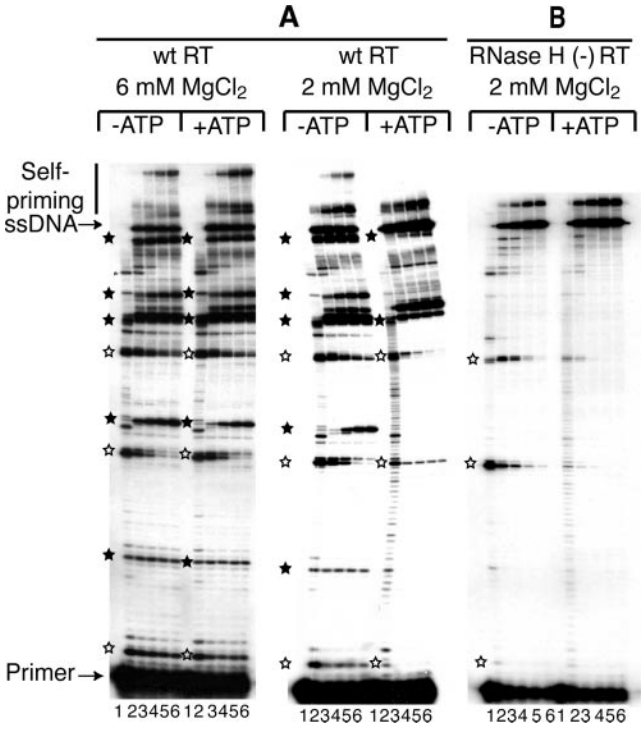

Figure 3. Influence of $MgCl_2$, ATP and RNase H activity on the accumulation of intermediate products. (**A**) PAGE analysis of the products generated by wt RT at 2 or 6 mM $MgCl_2$, in the absence or in the presence of 3.5 mM ATP. Transient (open stars) and dead-end (closed stars) intermediate products are indicated, together with the unextended primer, ssDNA and larger products produced by self-priming of ssDNA. (**B**) PAGE analysis of the products generated by E478Q RNase H(−) RT 2 mM $MgCl_2$, in the absence or in the presence of 3.5 mM ATP. Transient intermediate products are labeled as in A. Lanes 1–6 correspond to reverse transcription for 0, 1, 5, 10, 30 and 60 min.

mutant polymerase, irrespective of the presence of ATP (Figure 3B). As a result, ssDNA synthesis by RNase H(−) RT only slightly increased, from 46 to 49%, upon ATP addition and was more efficient than with wt RT (compare with Table 1). However, transient intermediate products were still observed in the absence of ATP (Figure 3B, open stars), confirming that transient and dead-end products have different origins. The latter ones requiring RNase H activity (Figure 3B), we suggest they are generated by rapid cleavage of the RNA template during a polymerization arrest, as observed by others (32). Cleaved RNA dissociates from the elongating DNA strand before RT can pass through the stop. A low free Mg^{2+} concentration might prevent the polymerase block by destabilizing the RNA structure or/and decrease the intrinsic RNase H activity.

To evaluate this hypothesis, we directly tested the influence of the $MgCl_2$ concentration and ATP on the RNase H activity of HIV-1 RT. Two modes of RNase H cleavage have been described: a polymerase-dependent cleavage (33), directed by the 3′ end of the DNA strand, and a polymerase-independent mechanism guided by the 5′ end of the RNA template (34). As the first mode of cleavage is thought to occur in concert with DNA polymerization to degrade the genomic RNA during (−) strand DNA synthesis, while the second may contribute to the degradation of larger genomic RNA fragments left after DNA 3′ end directed cleavage, we focussed on the polymerase-dependent RNase H activity. During polymerase-dependent cleavage, the RT polymerase active site is positioned at the recessed 3′ end of the DNA strand (Figure 4A). The RNase H active site is positioned at ~17 nt from the polymerase active site, and its position from the 3′ end of the DNA determines the position of the primary cleavage. RT then repositions and makes a secondary cleavage 7–9 nt from the recessed 3′ end of the DNA (Figure 4A).

We first tested polymerase-dependent cleavage using RNA1-47 as viral RNA and ODN35 as DNA. In this assay, the RNase H substrate is a 35mer RNA/DNA duplex with a 12 nt RNA overhang that has no predicted secondary structure. This assay is performed in the absence of dNTP, so that the structure of the substrate cannot be affected by polymerization. Thus, this assay reflects the influence of the $MgCl_2$ concentration on the intrinsic RNase H catalytic activity. The $MgCl_2$ concentration was varied from 1 to 6 mM, with and without 3.5 mM ATP. Under these conditions, cleavage of RNA1-47 followed first-order kinetics (data not shown). In the absence of ATP, the RNase H rate constant smoothly increased from 0.86 to 1.43 min^{-1} when the $MgCl_2$ concentration decreased from 6 to 2 mM, and it slightly decreased (to 1.23 min^{-1}) when the $MgCl_2$ concentration was further reduced to 1 mM (Figure 4B). Surprisingly, the RNase H rate constant followed the same trend in the presence of 3.5 mM ATP, and addition of ATP in the presence of 1 or 2 mM $MgCl_2$ had no significant effect on the intrinsic RNase H catalytic activity (Figure 4B), in sharp contrast with the polymerization rate constant (Figure 1). The most plausible explanation to the fact that ATP does not affect the RNase H activity is that the RNase H active site has a much higher affinity for Mg^{2+} ions than ATP, in agreement with recent crystallographic studies of a bacterial RNase H in the presence of a DNA/RNA substrate (9).

During ssDNA synthesis, $MgCl_2$ and ATP might also indirectly affect RNase H by modifying the stability of the RNA template and/or by affecting its refolding during DNA synthesis (31,32). Therefore, we directly followed degradation of RNA1-311 during ssDNA synthesis by using a 5′-labeled template (Figure 4C). At 2 mM $MgCl_2$ and in the absence of ATP, two types of cleavage products were observed. The first category are transient products that appeared early in the kinetics and partially or totally disappeared as DNA synthesis proceeded (Figure 4C, open stars). Further processing of these products during DNA polymerization proves that the RNA template did not dissociate from the growing DNA chain at these positions. A second class of RNA fragments accumulated (or at least did not disappear) during DNA synthesis (Figure 4C, black stars). At these positions, the cleaved RNA template might eventually dissociate from the nascent DNA chain, generating dead-end DNA products, as hypothesized earlier. Interestingly, cleavage of RNA1-311 was strongly reduced upon addition of ATP, and the products that accumulated in the absence of ATP almost completely disappeared, with the noticeable exception of the shortest (Figure 4C). Since the intrinsic RNase activity is unaffected by ATP at 2 mM $MgCl_2$ (Figure 4B), the inhibition of RNase H cleavage during ssDNA synthesis is most likely due to the influence of the free Mg^{2+} ion concentration on the RNA stability, structure and/or refolding.

Taken together, our data explain how reverse transcription of RNA1-311 increases at low concentration of free Mg^{2+} ions

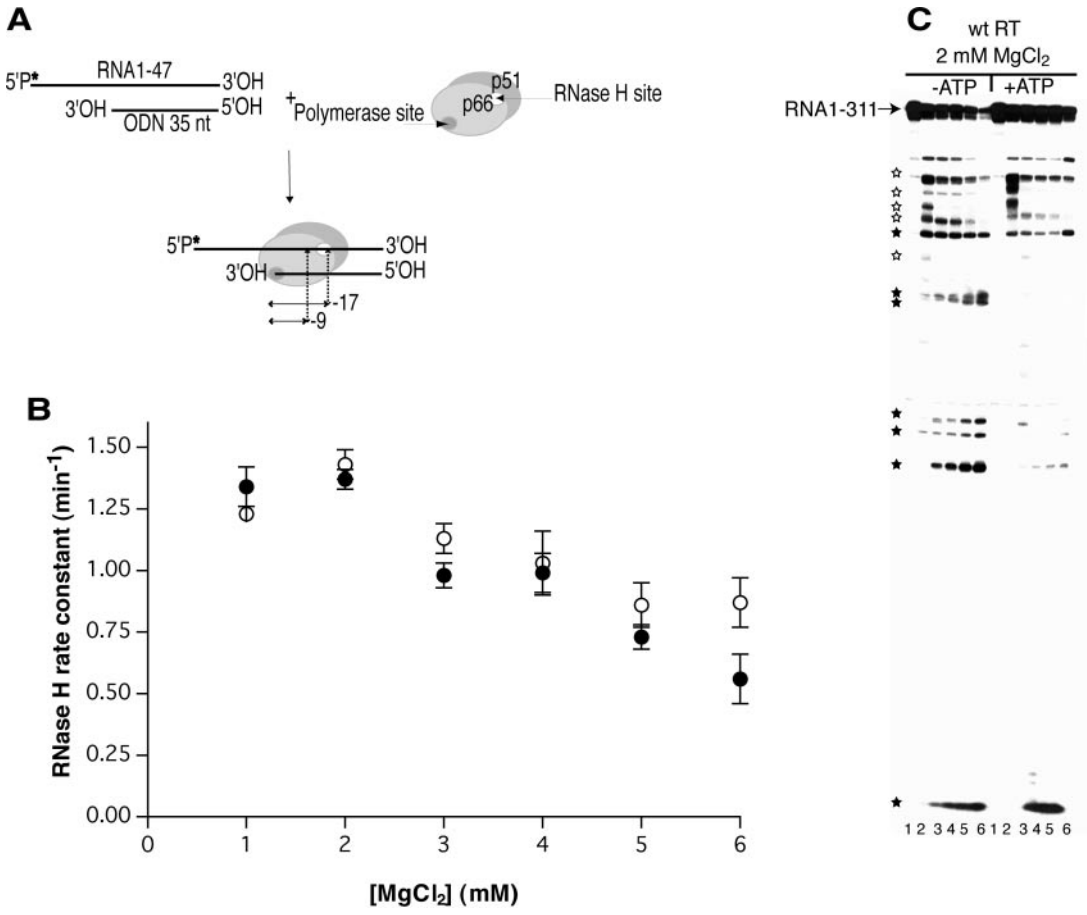

Figure 4. Influence of $MgCl_2$ and ATP on RNase H activity. (**A**) Schematic diagram of the polymerase-dependent RNase H cleavages and of the substrate used in (B). (**B**) The rate constant of RNase H cleavage of RNA1-47 in the absence (open circles) and in the presence (close circles) of 3.5 mM ATP is plotted as a function of the $MgCl_2$ concentration. (**C**) Cleavage of 5′-labeled RNA1-311 was followed during ssDNA synthesis in 2 mM $MgCl_2$, with or without 3.5 mM ATP. Lanes 1–6 correspond to reverse transcription for 0, 1, 5, 10, 30 and 60 min. Transient degradation products are marked by open stars, while those persisting or accumulating over time are indicated by closed stars.

(Figures 2 and 3, Tables 1 and 2) despite a strongly reduced intrinsic polymerase activity (Figure 1): low Mg^{2+} concentrations affect the RNA stability that indirectly decreases degradation of the RNA template by the RNase H activity (Figure 4), thus preventing premature dissociation of the template and primer strands that otherwise generates dead-end DNA products (Figure 3A). This model is supported by the observation that dead-end products are not generated by an RNase H(−) RT (Figure 3B).

The structural motifs present in RNA1-311 are found in the 5′ region of HIV-1 genomic RNA, and those located in R are most likely also present in the 3′ region of this RNA. Stable RNA secondary structures have also been identified in several coding regions of HIV-1 RNA including *gag* (27,35), *pol* (36) and *env* (37,38). Thus, reverse transcription of not only the 5′-untranslated region (5′-UTR), but also of the complete HIV-1 genomic RNA is likely to be strongly affected by variations in the free Mg^{2+} ion concentration. Indeed, since Mg^{2+} has a general stabilizing effect on RNA secondary and tertiary structures, increased RNase H cleavage of the template and dead-end product formation at high Mg^{2+} concentration should be a general phenomenon, even though we cannot predict the number and position of the cleavage sites.

Inhibition of ssDNA synthesis by NRTIs

In order to test the influence of the free Mg^{2+} ion concentration on the inhibition of reverse transcription by NRTIs, we compared ssDNA synthesis in the presence of the triphosphate form of FDA-approved NRTIs (3TCTP, AZTTP, ddATP the active metabolite of ddI, ddCTP and d4TTP), in the absence or presence of 3.5 mM ATP. These NRTIs compete with natural dNTPs, are incorporated into elongating DNA by HIV-1 RT and induce chain termination because they lack a 3′ hydroxyl group [for review, see Ref. (2)].

At 6 mM $MgCl_2$, ssDNA synthesis was inhibited by $\geqslant$85% with all NRTIs, except 3TCTP, which was slightly less efficient (54% inhibition) (Table 3), in agreement with its slow incorporation rate (39). The efficiency of these NRTIs slightly decreased in the presence of 2 mM $MgCl_2$ or 6 mM $MgCl_2$ and 3.5 mM ATP (Table 3). Remarkably, the NRTI efficiency was dramatically reduced in the presence of 2 mM $MgCl_2$ and 3.5 mM ATP (Table 3 and Figure 5). At 2 mM $MgCl_2$ and 3.5 mM ATP, ddATP, ddCTP, 3TCTP and d4TTP reduced ssDNA synthesis only by 15–38%, while AZTTP remained more efficient (62% inhibition). In all cases, more ssDNA was synthesized in the presence of NRTIs at 2 mM $MgCl_2$ and 3.5 mM ATP than in the absence of inhibitor at 6 mM $MgCl_2$ (Table 3).

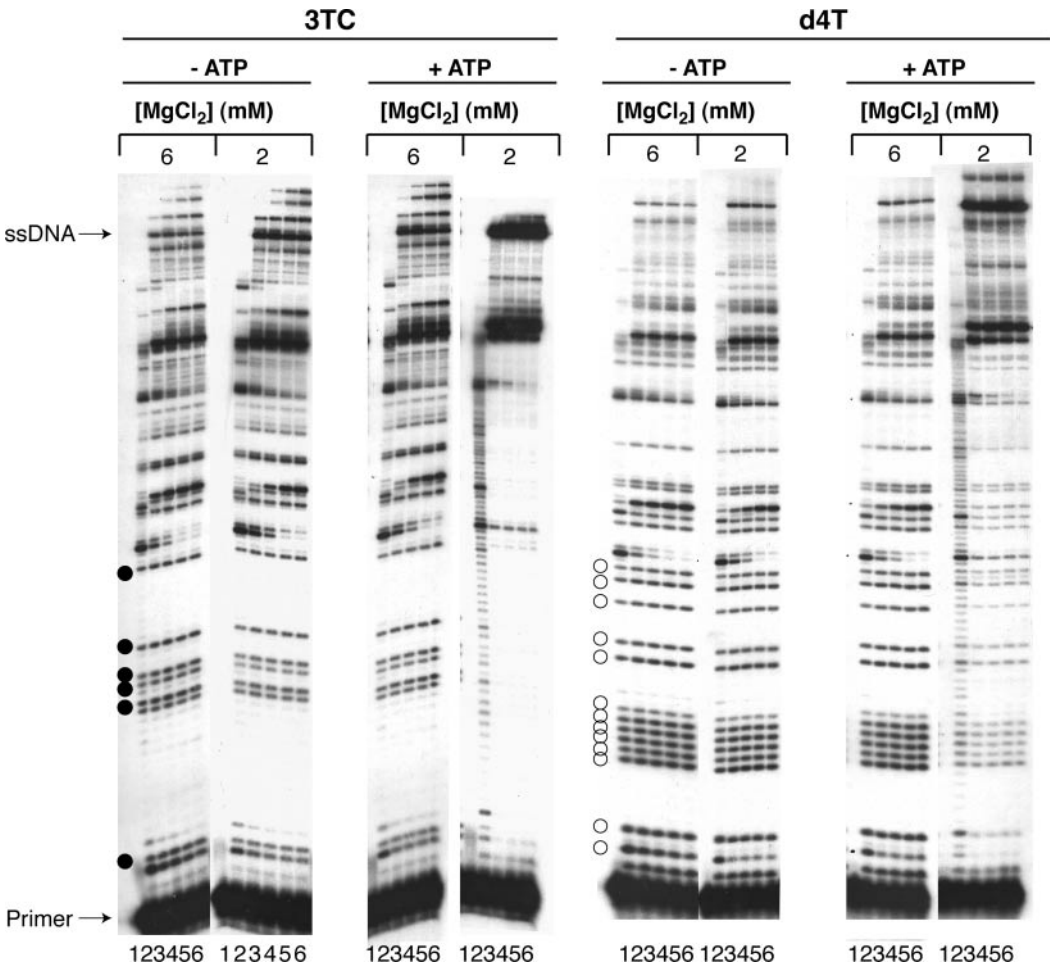

Figure 5. Influence of $MgCl_2$ and ATP on the inhibition of ssDNA synthesis by NRTIs. Synthesis of ssDNA was performed in the presence of 5 μM 3TCTP or d4TTP at 2 or 6 mM $MgCl_2$, in the absence or in the presence of 3.5 mM ATP. The first 6 3TC- and 13 d4T-incorporation sites are marked by closed and open circles, respectively. Lanes 1–6 correspond to reverse transcription for 0, 1, 5, 10, 30 and 60 min.

This was also true when RNase H(−) RT was substituted for wt RT, even though the mutant polymerase was more sensitive to NRTIs at all Mg^{2+} concentrations tested (Table 3). This indicates that the effect of ATP on RT discrimination against NRTIs is not due to an indirect effect on RNase H activity.

Kinetics of inhibition of ssDNA synthesis by NRTIs showed that the intensity of the bands corresponding to NRTI-terminated DNA molecules did not vary over time, indicating that once incorporated in the DNA chain, wt RT did not excise the nucleoside analogues by a PPi or ATP-dependent mechanism [for a review, see (20)] (Figure 5 and left panel of Figure 6A). However, the intensity of the NRTI-terminated products strongly decreased with decreasing free Mg^{2+} concentration and totally disappeared in the case of 3TCTP. These results indicate that HIV-1 RT discriminates more efficiently against 3′-deoxynucleoside analogues at low free Mg^{2+} concentration and are in line with a recent study by Deval *et al.* (19) showing that the K_m of Mg^{2+} for incorporation of AZTTP and d4TTP is 4-fold higher than that for dTTP. They indicate that the *in vivo* potency of NRTIs might be dramatically lower than deduced from *in vitro* assays performed at high Mg^{2+} concentration, owing to the low free Mg^{2+} concentration in several cell types, fluids and organs infected by HIV-1 (14–16).

As we looked at the inhibition of ssDNA synthesis by NRTIs, NRTI incorporation sites were located in different structural contexts: some were in loops or single-stranded stretches, whereas others were in stable helices. Despite this fact, our data (Figure 5 and data not shown) indicated that diminished NRTI incorporation at low concentration of free Mg^{2+} ions was a general phenomenon, taking place at all sites. Hence, increased discrimination against NRTIs at low Mg^{2+} concentration is most likely independent of the RNA structure.

To strengthen this conclusion, we studied discrimination between NRTIs and dNTPs using a short unstructured DNA template corresponding to the PBS and 20 nt 5′ of it. In agreement with previous studies (40), DNA synthesis appeared less processive on this DNA template than on RNA, especially at very low Mg^{2+} concentration. Distributive synthesis prevented accurate quantification of the NRTI incorporation at 2 mM $MgCl_2$ when ATP was present. Therefore, we compared discrimination between NRTIs (d4TTP or ddATP) and the corresponding dNTPs (dTTP or dATP) at 3 and 6 mM $MgCl_2$; with or without 3.5 mM ATP. As shown in Supplementary Figure 1 and quantified in Supplementary Table 1, adding 3.5 mM ATP during DNA synthesis had no significant effect on discrimination at 6 mM $MgCl_2$. However, at 2 mM $MgCl_2$, ATP increased discrimination between NRTIs and dNTPs by

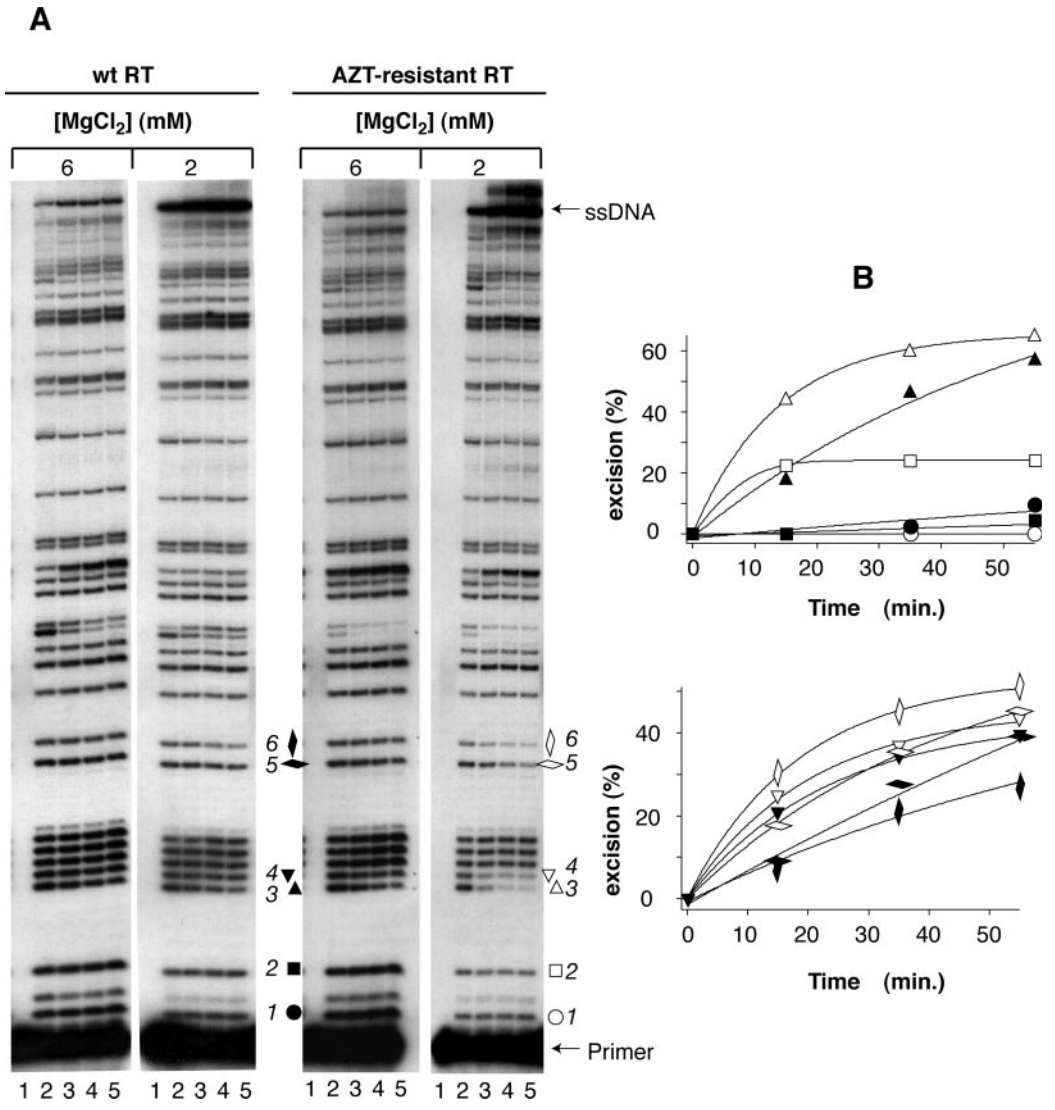

Figure 6. Influence of $MgCl_2$ and ATP on primer unblocking by AZT-resistant RT. (**A**) ssDNA synthesis was performed in the presence of 3.5 mM ATP and 4 μM AZTTP with wt or AZT-resistant RT at 2 or 6 mM $MgCl_2$. Six AZT incorporation sites that are analysed in (B) are numbered from 1 to 6 and marked by symbols. Lanes 1–5 correspond to reverse transcription for 0, 5, 20, 40 and 60 min. (**B**) Quantification of primer unblocking by AZT-resistant RT at the six incorporation sites marked in (A). The decrease of the band intensity relative to the first time point (5 min) is plotted against the reaction time.

1.5- to 2-fold. Thus, increased discrimination against NRTIs was observed both on a structured RNA or an unstructured DNA template. Discrimination was more pronounced on the RNA template, but this could be linked to the fact that higher $MgCl_2$ concentrations had to be used with the DNA template.

The increased discrimination against NRTIs at low Mg^{2+} concentration is not trivial to explain, as the two Mg^{2+} ions of the RT polymerase site interact with the phosphate groups of the incoming dNTP, but not with its 3′-hydroxyl group (3) (Figure 7). Thus, dNTPs and NRTIs probably bind Mg^{2+} with similar strength. The crystal structure of RT with a bound primer/template and an incoming dNTP showed that the deoxyribose and phosphate parts of the dNTP are maintained by three networks of interactions: (i) the 3′ hydroxyl group of the dNTP projects into a small pocket lined by the side chains of D113, Y115, F116 and Q151 (Figure 7, in blue) and the main-chain between 113 and 115 (Figure 7, blue and purple). It may

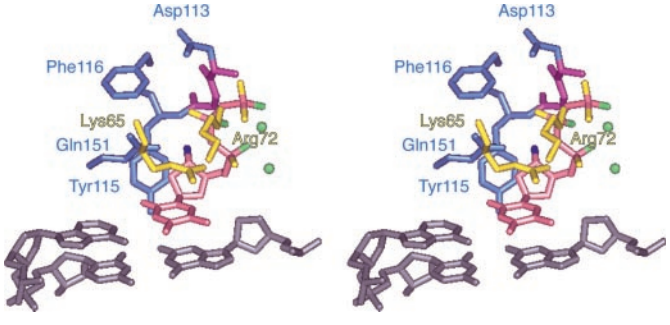

Figure 7. Stereo view of the interactions of the incoming dNTP in the polymerase site of HIV-1 RT. Part of the crystal structure solved by Huang *et al*. (3) is shown with the primer and template residues in gray, the core of the incoming dTTP in salmon, the two Mg^{2+} ions in green, the side chains of Asp113, Tyr115, Phe116 and Gln151 in blue, the side chains of Lys65 and Arg72 in yellow and the main chain of residues 113 and 114 (which belong to the blue and yellow sets) in purple.

also form an intramolecular H-bond with the pro-S_p oxygen of the β phosphate. (ii) The convex face of the triphosphate moiety is coordinated by the side chains of K65 (with the α phosphate) and R72 (with the γ phosphate) (Figure 7, in yellow), and the main-chain of residues 113 and 114 (Figure 7, purple). (iii) On the concave face, a non-bridging oxygen from each of the phosphate interacts with one Mg^{2+} ion, while the α phosphate also interacts with the other Mg^{2+} ion (Figure 7, in yellow) (3). Our data, together with previous studies, suggest that one of the interaction sets can be perturbed without drastic effects: (i) wt RT efficiently incorporates 2′,3′-dideoxynucleotides (ddNTP, including NRTIs) (41), (ii) mutation K65R has minimal effects on the incorporation of natural dNTPs (42) and (iii) RT is active at very low Mg^{2+} concentration (our results). However, simultaneously perturbing two interaction networks dramatically reduces activity: ddNTPs are not efficiently incorporated by K65R RT, which is thus resistant to several NRTIs (42), or by wt RT at low free Mg^{2+} concentration (our results). It seems that this activity decrease is due to a perturbation of the ddNTP conformation that affects the catalytic step, rather than reduced ddNTP binding (42).

Primer unblocking by AZT-resistant RT

Resistance to NRTIs involves two main mechanisms: increased discrimination against the inhibitor and primer unblocking by excision of the NRTI after its incorporation in the growing DNA chain (20). Excision is the main resistance mechanism against AZT and can also concern most other NRTIs, depending of the resistance mutations that are selected during viral replication (20). Prolonged treatments with AZT select for resistance mutations that allow excision of the incorporated AZTMP by using ATP as a pyrophosphate donor (20). To study the impact of the free Mg^{2+} concentration on the excision reaction, we compared the inhibition of ssDNA synthesis by AZTTP using either wt or an AZT-resistant RT bearing mutations D67N, K70R, T215F and K219Q at constant ATP (3.5 mM) and varying $MgCl_2$ concentrations (Figure 6). In the presence of 4 μM AZTTP, wt RT extended 3.2 and 9.5% of the primer into ssDNA at 6 and 2 mM $MgCl_2$, respectively, while ssDNA amounted to 6.4 and 18.9% at 6 and 2 mM $MgCl_2$, respectively, with AZT-resistant RT (Figure 6A).

As shown by PAGE, the intensity of the bands corresponding to AZTMP-terminated products did not vary over time with wt RT, while the intensity of some of these bands decreased at increasing reaction times with AZT-resistant RT, thus confirming that resistant RT, unlike wt RT, excised AZTMP at some specific positions (Figure 6A). Quantification of the time-course evolution of six representative AZT-terminated products showed that the excision efficiency greatly varied from one AZT incorporation site to the other (Figure 6B): it varied from ⩽5 to >60% unblocking after 1 h. However, this process was always more efficient at 2 mM than at 6 mM $MgCl_2$ (Figure 6B). This was unexpected since, *in vivo*, the excision mechanism most likely requires binding of ATP, or more precisely Mg(II)·ATP, into the RT polymerase active site (43,44).

In the case of AZTTP incorporation sites 3–6, we were able to show that the AZTMP excision followed first order kinetics and to determine the excision rate constants. The AZTMP excision rate constant increased by 1.42 (site 5) to 4.15 (site 6) fold as the $MgCl_2$ concentration decreased from 6 to 2 mM (data not shown). Thus, the influence of the $MgCl_2$ concentration on AZTMP excision is position dependent, suggesting a sequence-dependent or structure-dependent effect. Interestingly, NRTI excision was recently shown to be enhanced when the RNase H activity is diminished (45). It was proposed that after RNase H cleavage, the DNA growing strand dissociates from the template, thereby preventing AZTMP excision. In our case, increased excision might be the result of decreased RNase H activity at low free Mg^{2+} concentration, as observed in Figure 4C, which would provide more time for the ATP-lysis to take place before DNA dissociates from the degraded RNA template. Thus, reduced accumulation of dead-end products and enhanced AZTMP excision during ssDNA synthesis at low Mg^{2+} concentration probably have the same origin.

Concluding remarks

The Mg^{2+} concentrations in human lymphocytes (16), blood (15) and the brain (14) are much lower than those usually used in *in vitro* RT studies. Lymphocytes are one of the main HIV-1 targets, and reverse transcription already starts in biological fluids, inside the viral particles (46). In addition, HIV-1 often infects the brain (47). Therefore, it was important to evaluate the influence of the Mg^{2+} concentration on reverse transcription. Here, we systematically studied the effects of the Mg^{2+} concentration on the polymerase and RNase H activities of HIV-1 RT on synthetic and natural RNA templates, on the inhibition of reverse transcription by NRTIs, and on resistance to these drugs by primer unblocking. In order to mimic the cellular situation as closely as possible, we not only varied the $MgCl_2$ concentration, but also included a physiological ATP concentration in some of our experiments. Indeed, ATP and other cellular magnesium binders (NTP, dNTP, DNA, RNA) likely compete with RT for Mg^{2+} ions *in vivo*.

Our study demonstrated multiple influences of the free Mg^{2+} ion concentration on reverse transcription of a natural RNA template, its inhibition by NRTIs and excision of AZTMP after its incorporation in the DNA strand. The effects on the efficiency of reverse transcription and on resistance to AZT are most likely indirect and result from the influence of the free Mg^{2+} ion concentration on the RNase H activity, which is itself indirectly due to the influence of Mg^{2+} ions on the RNA structure. On the contrary, the Mg^{2+} concentration directly affects the discrimination between natural dNTPs and NRTIs. Thus, our study indicates that the free Mg^{2+} concentration is a crucial parameter to take into account when studying reverse transcription, its inhibition by NRTIs, or the resistance mechanisms. It also stresses the importance of mimicking the natural situation as closely as possible, since the influence of the $MgCl_2$ and ATP concentrations on ssDNA synthesis could not be anticipated from their effects on polymerase and RNase H activities in model systems. Of course, the conditions prevailing during reverse transcription *in vivo* are more complex than those we used in this study, and the efficiency of reverse transcription, its inhibition by NRTIs and resistance to this inhibition might be affected by cellular and/or viral proteins involved in the reverse transcription complex.

Finally, the intracellular free Mg^{2+} concentration might vary considerably between different cell types or during the cell cycle, as a result of variations in the NTP and messenger RNA pools, for instance. These fluctuations might strongly affect HIV-1 replication and its inhibition, and might play a role in the establishment of HIV-1 reservoirs.

SUPPLEMENTARY DATA

Supplementary Data are available at NAR Online.

ACKNOWLEDGEMENTS

This work was supported by grants from the 'Agence Nationale de Recherches sur le SIDA' (ANRS) to C.E. and R.M. Funding to pay the Open Access publication charges for this article was provided by ANRS.

Conflict of interest statement. None declared.

REFERENCES

1. Arts,E.J. and Le Grice,S.F. (1998) Interaction of retroviral reverse transcriptase with template-primer duplexes during replication. *Prog. Nucleic Acid Res. Mol. Biol.*, **58**, 339–393.
2. Gotte,M. (2004) Inhibition of HIV-1 reverse transcription: basic principles of drug action and resistance. *Expert Rev.Anti Infect. Ther.*, **2**, 707–716.
3. Huang,H., Chopra,R., Verdine,G.L. and Harrison,S.C. (1998) Structure of a covalently trapped catalytic complex of HIV-1 reverse transcriptase: implications for drug resistance. *Science*, **282**, 1669–1675.
4. Kaushik,N., Rege,N., Yadav,P.N., Sarafianos,S.G., Modak,M.J. and Pandey,V.N. (1996) Biochemical analysis of catalytically crucial aspartate mutants of human immunodeficiency virus type 1 reverse transcriptase. *Biochemistry*, **35**, 11536–11546.
5. Patel,H.P., Jacobo-Molina,A., Ding,J., Tantillo,C., Clark,A.D.J., Raag,R., Nanni,R.G., Hughes,S.H. and Arnold,E. (1995) Insights into DNA polymerization mechanisms from structure and function analysis of HIV-1 reverse transcriptase. *Biochemistry*, **34**, 5351–5363.
6. Cirino,N.M., Cameron,C.E., Smith,J.S., Rausch,J.W., Roth,M.J., Benkovic,S.J. and Le Grice,S.F. (1995) Divalent cation modulation of the ribonuclease functions of human immunodeficiency virus reverse transcriptase. *Biochemistry*, **34**, 9936–9943.
7. Klumpp,K., Hang,J.Q., Rajendran,S., Yang,Y., Derosier,A., Wong Kai In,P., Overton,H., Parkes,K.E., Cammack,N. and Martin,J.A. (2003) Two-metal ion mechanism of RNA cleavage by HIV RNase H and mechanism-based design of selective HIV RNase H inhibitors. *Nucleic Acids Res.*, **31**, 6852–6859.
8. Davies,J.F.,II, Hostomska,Z., Hostomsky,Z., Jordan,S.R. and Matthews,D.A. (1991) Crystal structure of the ribonuclease H domain of HIV-1 reverse transcriptase. *Science*, **252**, 88–95.
9. Nowotny,M., Gaidamakov,S.A., Crouch,R.J. and Yang,W. (2005) Crystal structures of RNase H Bound to an RNA/DNA hybrid: substrate specificity and metal-dependent catalysis. *Cell*, **121**, 1005–1016.
10. Hoffman,A.D., Banapour,B. and Levy,J.A. (1985) Characterization of the AIDS-associated retrovirus reverse transcriptase and optimal conditions for its detection in virions. *Virology*, **147**, 326–335.
11. Rey,M.A., Spire,B., Dormont,D., Barre-Sinoussi,F., Montagnier,L. and Chermann,J.C. (1984) Characterization of the RNA dependent DNA polymerase of a new human T-lymphotropic retrovirus (lymphadenopathy associated virus). *Biochem. Biophys. Res. Commun.*, **121**, 126–133.
12. Starnes,M.C. and Cheng,Y.C. (1989) Human immunodeficiency virus reverse transcriptase-associated RNase H activity. *J. Biol. Chem.*, **264**, 7073–7077.
13. Wondrak,E.M., Lower,J. and Kurth,R. (1986) Functional purification and enzymic characterization of the RNA-dependent DNA polymerase of human immunodeficiency virus. *J. Gen. Virol.*, **67**, 2791–2797.
14. Gee,J.B.,II, Corbett,R.J.T., Perlman,J.M. and Laptook,A.R. (2001) Hypermagnesia does not increase brain intracellular magnesium in newborn swine. *Pediatr. Neurol.*, **25**, 304–308.
15. Wang,S., McDonnell,E.H., Sedor,F.A. and Toffaletti,J.G. (2002) pH effects on measurements of ionized calcium and ionized magnesium in blood. *Arch. Pathol. Lab. Med.*, **126**, 947–950.
16. Delva,P., Pastori,C., Degan,M., Montesi,G. and Lechi,A. (2004) Catecholamine-induced regulation *in vitro* and *ex vivo* of intralymphocyte ionized magnesium. *J. Membr. Biol.*, **199**, 163–171.
17. Smith,A.J., Meyer,P.R., Asthana,D., Ashman,M.R. and Scott,W.A. (2005) Intracellular substrates for the primer-unblocking reaction by human immunodeficiency virus type 1 reverse transcriptase: detection and quantitation in extracts from quiescent- and activated-lymphocyte subpopulations. *Antimicrob. Agents Chemother.*, **49**, 1761–1769.
18. Gallant,J.E., Gerondelis,P.Z., Wainberg,M.A., Shulman,N.S., Haubrich,R.H., St Clair,M., Lanier,E.R., Hellmann,N.S. and Richman,D.D. (2003) Nucleoside and nucleotide analogue reverse transcriptase inhibitors: a clinical review of antiretroviral resistance. *Antivir. Ther.*, **8**, 489–506.
19. Deval,J., Alvarez,K., Selmi,B., Bermond,M., Boretto,J., Guerreiro,C., Mulard,L. and Canard,B. (2005) Mechanistic insights into the suppression of drug resistance by human immunodeficiency virus type 1 reverse transcriptase using alpha-boranophosphate nucleoside analogs. *J. Biol. Chem.*, **280**, 3838–3846.
20. Goldschmidt,V. and Marquet,R. (2004) Primer unblocking by HIV-1 reverse transcriptase and resistance to nucleoside RT inhibitors (NRTIs). *Int. J. Biochem. Cell. Biol.*, **36**, 1687–1705.
21. Marquet,R., Baudin,F., Gabus,C., Darlix,J.L., Mougel,M., Ehresmann,C. and Ehresmann,B. (1991) Dimerization of human immunodeficiency virus (type 1) RNA: stimulation by cations and possible mechanism. *Nucleic Acids Res.*, **19**, 2349–2357.
22. Le Grice,S.F., Cameron,C.E. and Benkovic,S.J. (1995) Purification and characterization of human immunodeficiency virus type 1 reverse transcriptase. *Methods Enzymol.*, **262**, 130–144.
23. Didierjean,J., Isel,C., Querre,F., Mouscadet,J.F., Aubertin,A.M., Valnot,J.Y., Piettre,S.R. and Marquet,R. (2005) Inhibition of Human Immunodeficiency Virus Type 1 Reverse Transcriptase, RNase H, and Integrase Activities by Hydroxytropolones. *Antimicrob. Agents Chemother.*, **49**, 4884–4894.
24. Cristofaro,J.V., Rausch,J.W., Le Grice,S.F. and DeStefano,J.J. (2002) Mutations in the ribonuclease H active site of HIV-RT reveal a role for this site in stabilizing enzyme-primer-template binding. *Biochemistry*, **41**, 10968–10975.
25. Tan,C.K., Zhang,J., Li,Z.Y., Tarpley,W.G., Downey,K.M. and So,A.G. (1991) Functional characterization of RNA-dependent DNA polymerase and RNase H activities of a recombinant HIV reverse transcriptase. *Biochemistry*, **30**, 2651–2655.
26. Ding,J., Das,K., Hsiou,Y., Sarafianos,S.G., Clark,A.D.J., Jacobo-Molina,A., Tantillo,C., Hughes,S.H. and Arnold,E. (1998) Structure and functional implications of the polymerase active site region in a complex of HIV-1 RT with a double-stranded DNA template-primer and an antibody Fab fragment at 2.8 A resolution. *J. Mol. Biol.*, **284**, 1095–1111.
27. Baudin,F., Marquet,R., Isel,C., Darlix,J.L., Ehresmann,B. and Ehresmann,C. (1993) Functional sites in the 5′ region of human immunodeficiency virus type 1 RNA form defined structural domains. *J. Mol. Biol.*, **229**, 382–397.
28. Paillart,J.C., Dettenhofer,M., Yu,X.F., Ehresmann,C., Ehresmann,B. and Marquet,R. (2004) First snapshots of the HIV-1 RNA structure in infected cells and in virions. *J. Biol. Chem.*, **279**, 48397–48403.
29. Lanciault,C. and Champoux,J.J. (2005) Effects of unpaired nucleotides within HIV-1 genomic secondary structures on pausing and strand transfer. *J. Biol. Chem.*, **280**, 2413–2423.
30. Suo,Z. and Johnson,K.A. (1997) Effect of RNA secondary structure on the kinetics of DNA synthesis catalyzed by HIV-1 reverse transcriptase. *Biochemistry*, **36**, 12459–12467.
31. Suo,Z. and Johnson,K.A. (1997) RNA secondary structure switching during DNA synthesis catalyzed by HIV-1 reverse transcriptase. *Biochemistry*, **36**, 14778–14785.
32. Suo,Z. and Johnson,K.A. (1997) Effect of RNA secondary structure on RNA cleavage catalyzed by HIV-1 reverse transcriptase. *Biochemistry*, **36**, 12468–12476.
33. Gopalakrishnan,V., Peliska,J.A. and Benkovic,S.J. (1992) Human immunodeficiency virus type 1 reverse transcriptase: spatial and temporal

relationship between the polymerase and RNase H activities. *Proc. Natl Acad. Sci. USA*, **89**, 10763–10767.
34. Wisniewski,M., Balakrishnan,M., Palaniappan,C., Fay,P.J. and Bambara,R.A. (2000) Unique progressive cleavage mechanism of HIV reverse transcriptase RNase H. *Proc. Natl Acad. Sci. USA*, **97**, 11978–11983.
35. Paillart,J.C., Skripkin,E., Ehresmann,B., Ehresmann,C. and Marquet,R. (2002) *In vitro* evidence for a long range pseudoknot in the 5′-untranslated and matrix coding regions of HIV-1 genomic RNA. *J. Biol. Chem.*, **277**, 5995–6004.
36. Parkin,N.T., Chamorro,M. and Varmus,H.E. (1992) Human immunodeficiency virus type 1 gag-pol frameshifting is dependent on downstream mRNA secondary structure: demonstration by expression *in vivo*. *J. Virol.*, **66**, 5147–5151.
37. Heaphy,S., Dingwall,C., Ernberg,I., Gait,M.J., Green,S.M., Karn,J., Lowe,A.D., Singh,M. and Skinner,M.A. (1990) HIV-1 regulator of virion expression (Rev) protein binds to an RNA stem–loop structure located within the Rev response element region. *Cell*, **60**, 685–693.
38. Peleg,O., Brunak,S., Trifonov,E.N., Nevo,E. and Bolshoy,A. (2002) RNA secondary structure and squence conservation in C1 region of human immunodeficiency virus type 1 env gene. *AIDS Res. Hum. Retroviruses*, **18**, 867–878.
39. Krebs,R., Immendorfer,U., Thrall,S.H., Wohrl,B.M. and Goody,R.S. (1997) Single-step kinetics of HIV-1 reverse transcriptase mutants responsible for virus resistance to nucleoside inhibitors zidovudine and 3-TC. *Biochemistry*, **36**, 10292–10300.
40. Huber,H.E., McCoy,J.M., Seehra,J.S. and Richardson,C.C. (1989) Human immunodeficiency virus 1 reverse transcriptase. Template binding, processivity, strand displacement synthesis, and template switching. *J. Biol. Chem.*, **264**, 4669–4678.
41. Dahlberg,J.E., Mitsuya,H., Blam,S.B., Broder,S. and Aaronson,S.A. (1987) Broad spectrum antiretroviral activity of 2′,3′-dideoxynucleosides. *Proc. Natl Acad. Sci. USA*, **84**, 2469–2473.
42. Selmi,B., Boretto,J., Sarfati,S.R., Guerreiro,C. and Canard,B. (2001) Mechanism-based suppression of dideoxynucleotide resistance by K65R human immunodeficiency virus reverse transcriptase using an alpha-boranophosphate nucleoside analogue. *J. Biol. Chem.*, **276**, 48466–48472.
43. Boyer,P.L., Sarafianos,S.G., Arnold,E. and Hughes,S.H. (2001) Selective excision of AZTMP by drug-resistant human immunodeficiency virus reverse transcriptase. *J. Virol.*, **75**, 4832–4842.
44. Meyer,P.R., Matsuura,S.E., Mian,A.M., So,A.G. and Scott,W.A. (1999) A mechanism of AZT resistance: an increase in nucleotide-dependent primer unblocking by mutant HIV-1 reverse transcriptase. *Mol. Cell*, **4**, 35–43.
45. Nikolenko,G.N., Palmer,S., Maldarelli,F., Mellors,J.W., Coffin,J.M. and Pathak,V.K. (2005) Mechanism for nucleoside analog-mediated abrogation of HIV-1 replication: Balance between RNase H activity and nucleotide excision. *Proc. Natl Acad. Sci. USA*, **102**, 2093–2098.
46. Zhang,H., Dornadula,G. and Pomerantz,R.J. (1998) Natural endogenous reverse transcription of HIV-1. *J. Reprod. Immunol.*, **41**, 255–260.
47. Berger,J.R. and Avison,M. (2004) The blood brain barrier in HIV infection. *Front. Biosci.*, **9**, 2680–2685.